



# Study of D<sub>2</sub>O/H<sub>2</sub>O-cooled thorium-fueled PWR-like SMR cores using the KNACK toolbox: conversion and safety assessment

Alexis Nuttin, Nicolas Capellan, Olivier Méplan, Pierre Prévot

## ► To cite this version:

Alexis Nuttin, Nicolas Capellan, Olivier Méplan, Pierre Prévot. Study of D<sub>2</sub>O/H<sub>2</sub>O-cooled thorium-fueled PWR-like SMR cores using the KNACK toolbox: conversion and safety assessment. International Congress on Advances in Nuclear Power Plants (ICAPP 2019), 2019, Juan les pins, France.  
hal-03782798

HAL Id: hal-03782798

<https://hal.science/hal-03782798>

Submitted on 22 Sep 2022

**HAL** is a multi-disciplinary open access archive for the deposit and dissemination of scientific research documents, whether they are published or not. The documents may come from teaching and research institutions in France or abroad, or from public or private research centers.

L'archive ouverte pluridisciplinaire **HAL**, est destinée au dépôt et à la diffusion de documents scientifiques de niveau recherche, publiés ou non, émanant des établissements d'enseignement et de recherche français ou étrangers, des laboratoires publics ou privés.

## Study of D<sub>2</sub>O/H<sub>2</sub>O-cooled thorium-fueled PWR-like SMR cores using the KNACK toolbox: conversion and safety assessment

A. Nuttin<sup>1,\*</sup>, N. Capellan<sup>1</sup>, O. Méplan<sup>1</sup>, P. Prévot<sup>1</sup>

<sup>1</sup>LPSC, Université Grenoble-Alpes, CNRS/IN2P3, Grenoble, France

\*Corresponding Author, E-mail: alexis.nuttin@lpsc.in2p3.fr

**KEYWORDS:** Thorium, Heavy Water, Spectral Shift Control, Small Modular Reactor

Based on SMURE (Serpent2/MCNP Utility) and NDM (Nodal Drift Method for time-dependent diffusion), a full set of academic methods named KNACK (Knack of Nodal Approach to Core Kinetics) has been used for the design of 600 MW<sub>th</sub> D<sub>2</sub>O/H<sub>2</sub>O-cooled thorium-fueled SMR (Small Modular Reactor) cores. Three types of lattice, with 17x17, 19x19 or 21x21 PWR-like FAs (Fuel Assemblies), have been considered. After initial fissile zoning for power flattening, full core burnup calculations with D<sub>2</sub>O/H<sub>2</sub>O Spectral Shift Control have been performed at HFP (Hot Full Power) for the comparison of conversion performance. Temperature dependences of diffusion data have been implemented within a thermal lumped model for safety. A simple criterion, on coolant temperatures only, has finally been used for the comparative analysis of Rod Ejection Accidents (REA) from HZP (Hot Zero Power).

### I. Introduction

In the frame of our Simulation Initiative for Reactors Improving Uranium savings and Safety margins (SIRIUS), a few first burnup calculations of water-cooled thorium-fueled options have given promising conversion results<sup>1</sup>. Fully exploiting the version 2 of Serpent<sup>2</sup> for core calculations, our new C++ framework SMURE<sup>3</sup> has been completed by a nodal method for spatial kinetics called NDM<sup>4,5</sup>. All these simple methods, including thermal models, have been arranged in a toolbox named KNACK, mainly for the design of light water-cooled thorium-fueled SMR cores with reduced soluble boron and burnable poisons<sup>6,7</sup>. In parallel and in a quite simplified way, we have also explored the potential of Spectral Shift Control (SSC) by H<sub>2</sub>O additions in an initial D<sub>2</sub>O coolant<sup>8</sup>. Together with a first compact description of KNACK, these studies of D<sub>2</sub>O/H<sub>2</sub>O-cooled SMR cores are summarized in this paper.

### II. Basic core design and burnup calculations

Our main design choices are based either on recent SMR studies or on historical experiments. Two detrimental effects on fuel utilization in SMR<sup>9</sup> are addressed: *neutron leakage* is reduced by a ThO<sub>2</sub> blanket and *burnable poisons* are replaced by D<sub>2</sub>O/H<sub>2</sub>O SSC for reactivity management (as already simulated in our previous water-cooled core studies<sup>1</sup>). Single-batch fuel scheme is maintained for its simplicity<sup>10</sup>, and (Th/<sup>233</sup>U)O<sub>2</sub> is chosen as a convenient fuel (close to its equilibrium). Simple geometry and power considerations<sup>11</sup> lead to a typical core (cf. Fig. 1) similar to the small (Th/<sup>233</sup>U)O<sub>2</sub>-fueled core of the Indian Point PWR<sup>12</sup> and using SSC as tested by the historical SSCR experiment<sup>13</sup>.

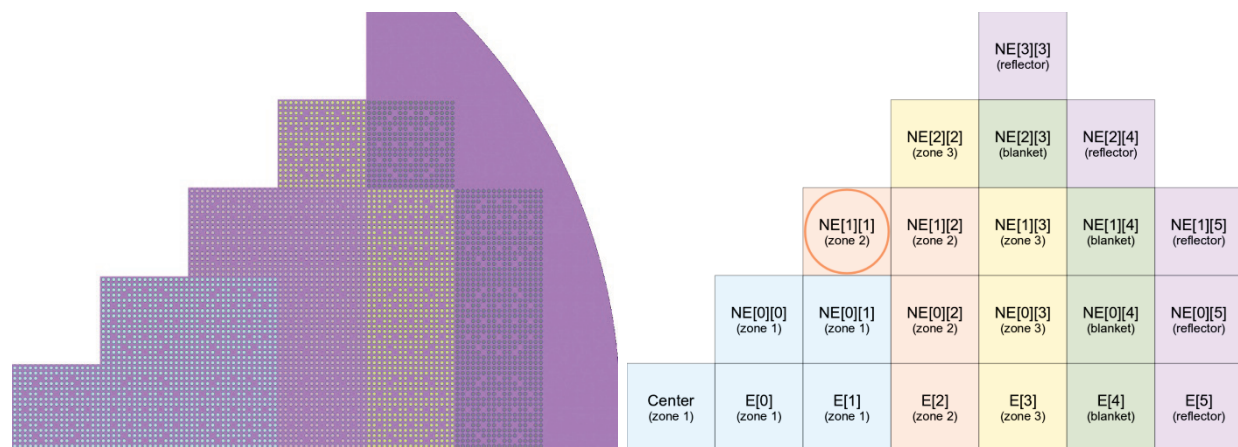


Fig. 1. Radial geometries (E-NE octant only) used for SMURE burnup (left) and NDM transient (right) calculations.

A unique core structure of 69 2.0-m high ( $\text{Th}/^{233}\text{U}$ ) $\text{O}_2$ -fueled FAs surrounded by a  $\text{ThO}_2$  blanket is used. Here we detail how cores are sized and zoned at BOC (Beginning Of Cycle) for optimal nominal conditions in each case, then we compare burnup results obtained by FCU (Full Core evolution with few Universes). For all these steps, a trade-off between spatial detail and computation time is found in dividing the core in 4 annular clusters of FAs (so-called “zones” in the following, cf. Fig. 1). Only the 3 most inner zones (numbered 1, 2 and 3) of respectively 21, 24 and 24 FAs are ( $\text{Th}/^{233}\text{U}$ ) $\text{O}_2$ -fueled.

With 28 FAs, zone 4 is the radial  $\text{ThO}_2$  blanket which replaces part of neutron leakage by some extra  $^{233}\text{U}$  production. Last but not least, the 20-cm thick axial and radial reflectors are considered as part of the primary circuit and have thus the same composition as the coolant, which is almost pure  $\text{D}_2\text{O}$  at BOC and then evolves as a  $\text{D}_2\text{O}/\text{H}_2\text{O}$  mix due to chosen SSC. These reflectors allow to keep leakage probability almost constant at about 5% in all cases. Let us specify that while the radial reflector ends at an external radius of 1.37 m for our SMURE burnup calculations, it is simply made of 32 water-filled FAs in our NDM model for transient calculations. NDM’s part of Fig. 1 shows from which zone 2’s FA, named NE[1][1] and indicated by a circle, a control cluster will be ejected in our REA studies.

## II.A. Power flattening by fissile zoning at BOC

The same total power of 600 MW<sub>th</sub> is imposed to all cores. Fuel volumic powers amount to about 300, 250 and 200 W/cc in the 17x17, 19x19 and 21x21 cases respectively (cf. Fig. 2). Radial profiles are flattened at BOC by zoning enrichments (with 4.0-6.0-8.0, 6.0-8.0-10.0 and 7.5-9.5-11.5 at% of  $^{233}\text{U}$  in HN for zones 1-2-3 of the 17x17, 19x19 and 21x21 cores respectively). From these BOC, evolution calculations have been performed using the FCU method of SMURE, with one single average fuel cell (and multigroup flux) computed by Serpent 2 per zone. Despite its simplicity, this validated method<sup>6,7</sup> quickly provides quite accurate results for these purposely annular-shaped zones. For fair comparison, the same EOC (End of Cycle), corresponding to about 1 GW<sub>e.y</sub>, is set for all cores to 5 years (EFPY).

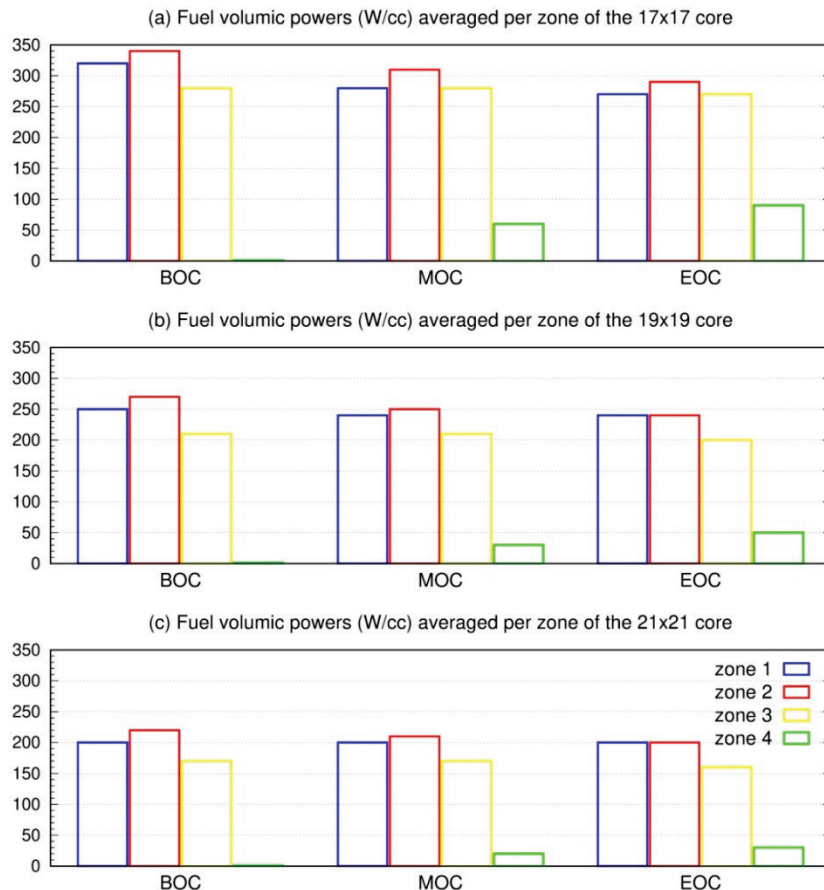


Fig. 2. Zone-averaged fuel volumic power profiles compared at BOC, MOC (Middle Of Cycle, at 2.5 y) and EOC.

## II.B. Comparison of final conversion performance

For SSC, a simple algorithm manages the semi-continuous replacement of  $D_2O$  by  $H_2O$ . After each of the five first MC steps (between two Serpent runs) of 1, 4, 5, 10 and 20 days,  $H_2O$  is added in the coolant at a constant rate (of +0.01 at% per day in the 17x17 case). Then each new add is adjusted: if last  $k_{eff}$  is greater (resp. lower) than both 1 and second to last  $k_{eff}$  i.e. increasing (resp. decreasing), it is simply decreased (resp. increased) by 0.05 at% in all cases. By keeping constant the total number of molecules per cc of coolant, its density is carefully updated. As shown by Fig. 3(a), spectra in fuel at BOC are clearly harder than in standard PWR,  $D_2O$  being much less efficient than  $H_2O$  as a moderator in such tight lattices. Fig. 3(b) shows in the 17x17 case that, along the whole cycle, our simulated SSC allows to improve moderation and thus to manage reactivity (cf. Fig. 4) without any other method.

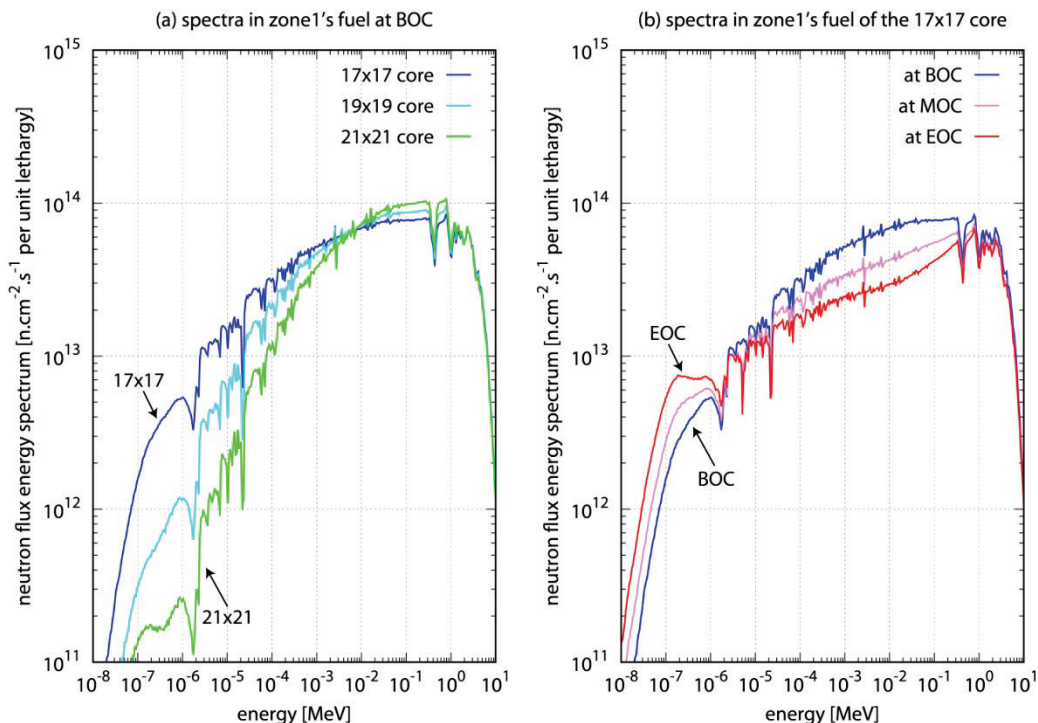


Fig. 3. Dependence of neutron flux energy spectra in zone 1's fuel on core lattice (a) and on burnup level (b).

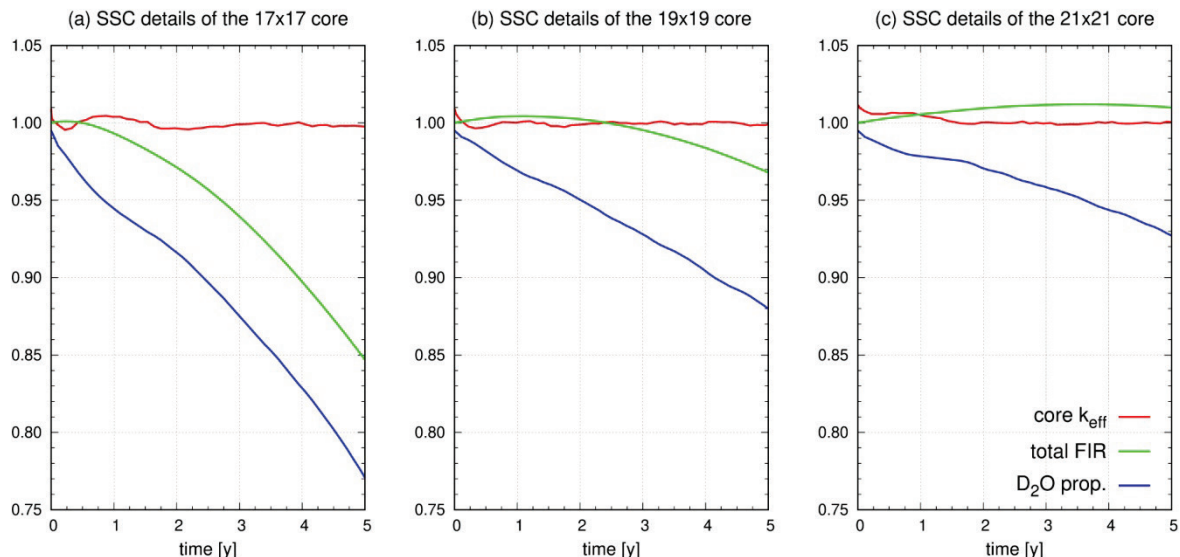


Fig. 4. Detailed time-evolution of key parameters for  $D_2O/H_2O$  SSC over the 5-y cycle common to the three cores.

In addition to the well-stabilized  $k_{\text{eff}}$  evolutions (in red), Fig. 4 shows how evolves in each case the FIR (Fissile Inventory Ratio). At any time  $t$ , FIR is defined here as the ratio of the “total fissile inventory” (including  $^{233}\text{U}$ ,  $^{235}\text{U}$  and  $^{233}\text{Pa}$  considered fully decayed into  $^{233}\text{U}$  as if  $t$  was EOC) over its initial value (i.e. the initial  $^{233}\text{U}$  inventory). After the same 5-y single-batch cycle, FIR amounts for the 17x17, 19x19 and 21x21 cases to 0.85, 0.97 and 1.01 respectively: lattice sub-moderation improves conversion so well that it even makes the 21x21 core slightly breed (without considering  $^{233}\text{Pa}$  decay, FIR is still 1.00 in this case). Last but not least, since dealing with the practical question of costly  $\text{D}_2\text{O}$  recovery for the next cycle, is shown the evolution of  $\text{D}_2\text{O}$  proportion (from 99.5 at% at BOC) in the coolant. Fig. 4(c) shows that the great moderating efficiency of  $\text{H}_2\text{O}$  limits its necessary proportion to only 7 at% at the 21x21 EOC. As shown by Fig. 3(b) in the 17x17 case and due to increasing 1-g fission cross sections, spectrum softening goes along with a total flux decrease (from 7.4 to  $4.5 \cdot 10^{14} \text{ cm}^{-2} \cdot \text{s}^{-1}$ ). Let us specify here that spectrum normalization has been made simple using SMURE GUI, a constant lethargy width for all groups and Serpent 2’s special detector type -3 (for division by lethargy width). Zone 2 and 3’s spectra closely look like zone 1’s, while zone 4’s are much softer with clear thermal humps (since there is no fissile absorption at BOC in this  $\text{ThO}_2$  blanket).

Last important conversion results are final burnup values, to be compared at same EOC. It is easy to anticipate that lattice sub-moderation, by increasing fuel inventory, reduces final burnup. But tricky to predict how much this effect is compensated by spectrum hardening, so let us have a look at Tab. 1 showing detailed burnup results from our SMURE calculations. For each core, the first column gives final burnup computed over all zones (zone 4 included) and the corresponding HN (Heavy Nuclei) inventory. Compared to 17x17 burnup close to 50 GWd/t, 21x21’s one is almost reduced to 30 GWd/t because of its fuel loading higher by almost 50%. In order to give more representative results, Tab. 1’s second column focuses on the fissile part of each core (completed by last column on blanket). Simple weighting of burnup from these last two columns by their HN inventory gives back full core burnup. It is also possible, for instance, to estimate the proportion of total energy production in blanket to about 7%, 5% and only 3% in the 17x17, 19x19 and 21x21 cases respectively. In the same order, initial  $^{233}\text{U}$  inventories are 1.00, 1.68 and 2.46 (metric) tons. The 21x21 slight breeding is thus associated with a significantly increased  $^{233}\text{U}$  inventory at BOC. Particularly useful on leakage reduction (to a constant proportion of about 5% in all cases), zone 4 plays an essential role for conversion too. In all cases, it is the only zone which effectively produces  $^{233}\text{U}$  with 0.10, 0.12 and 0.14 tons (in usual order) at EOC.

	<b>full core</b> (zones 1 to 4)		<b>fissile core</b> (zones 1 to 3)		<b>blanket</b> (zone 4)	
	5-y burnup	HN inventory	5-y burnup	HN inventory	5-y burnup	HN inventory
<b>17x17</b>	48.4 GWd/t	22.8 tons	63.4 GWd/t	16.2 tons	11.5 GWd/t	6.6 tons
<b>19x19</b>	38.0 GWd/t	29.1 tons	51.0 GWd/t	20.7 tons	6.0 GWd/t	8.4 tons
<b>21x21</b>	30.6 GWd/t	36.0 tons	41.8 GWd/t	25.6 tons	3.2 GWd/t	10.4 tons

Tab. 1. Detailed burnup performance (w/ and w/o blanket) of each core at the end of the common 5-y cycle.

Interesting comparisons can be made with previous studies<sup>1</sup> on standard N4-type  $\text{H}_2\text{O}$ -cooled PWR cores homogeneously loaded with same fuel (at lower enrichment of about 3.5 at% of  $^{233}\text{U}$  in HN). In its 21x21 version, this core gets only 0.80 as FIR after a similar final burnup (of 33 GWd/t). The 17x17 version has similar final burnup (50 GWd/t) and way lower FIR (0.56) too, which emphasizes the great potential of  $\text{D}_2\text{O}/\text{H}_2\text{O}$  SSC (with a quite acceptable, limited proportion of  $\text{H}_2\text{O}$  at EOC).

### III. Extra methods for thermal details at HFP

In order to complete their previously described conversion results, all cores shall be tested against REA from HZP. For that purpose, NDM must be fed with 2-g FA-homogenized cross sections from Serpent 2. Dependence of these diffusion data on temperatures is simply interpolated for further use within a thermal lumped coupling. Then, as a prior test (and because it will be used in our single safety criterion), each HFP equilibrium is computed according to a basic methodology (described here as lightly as possible). It relies on a common coolant mass flow  $F_{\text{cool}}$  (of  $50 \text{ kg.s}^{-1}$  per FA) and, for each case, on the iterative determination of a global fuel-to-coolant conductance  $G_{\text{fuel}}$  (of a few  $10^4 \text{ W.K}^{-1}$ ).

### III.A. Temperature dependence of diffusion data

Diffusion data of each zone (7 cross sections and 2 velocities, cf. Tab. 2) are computed by Serpent 2 according to the usual NDM approximations<sup>4</sup> on three cores with unique fuel and coolant temperatures ( $T_{fuel}$ ,  $T_{cool}$ ) = (560, 560) corresponding to HZP, (1200, 560) or (560, 610) in K. The Relative Changes of these diffusion data vs.  $T_{fuel}$  and  $T_{cool}$  (resp. RCFT and RCCT) are obtained at the same time and indicated in Tab. 2 as well. In Serpent's inputs are only changed nuclide codes for  $T_{fuel}$  and, for  $T_{cool}$ , the coolant density (0.83 g/cc at 560 K, 0.69 g/cc at 610 K close to boiling point at BOC for almost pure D<sub>2</sub>O). In addition to zones 1 to 5 (20-cm thick water reflector), a rodded part of zone 2 merging the 4 [1][1] FAs fully filled with clusters of 24 B<sub>4</sub>C rods (N4 PWR-like<sup>14</sup>, except a 90 at% enrichment of B in <sup>10</sup>B) is detailed for REA. Only 4 (resp. 7) of the 9 RCFT's (resp. RCCT's) have been carefully checked to systematically have a non-zero value with respect to the sufficient precision of  $\pm 1$  pcm/K (resp.  $\pm 100$  pcm/K or 1 mk/K). Others, compatible with zero, are indicated as "(0)" in Tab. 2 below.

	Group 1 (above 0.625 eV)					Group 2			
	$\Sigma_{tr1}$	$v_1$	$\Sigma_{a1}$	$v\Sigma_{f1}$	$\Sigma_{12}$	$\Sigma_{tr2}$	$v_2$	$\Sigma_{a2}$	$v\Sigma_{f2}$
<b>value</b> at HZP	$2.55 \cdot 10^{-1}$ [cm <sup>-1</sup> ]	$2.86 \cdot 10^7$ [cm.s <sup>-1</sup> ]	$9.38 \cdot 10^{-3}$ [cm <sup>-1</sup> ]	$9.47 \cdot 10^{-3}$ [cm <sup>-1</sup> ]	$7.37 \cdot 10^{-4}$ [cm <sup>-1</sup> ]	$3.67 \cdot 10^{-1}$ [cm <sup>-1</sup> ]	$5.94 \cdot 10^5$ [cm.s <sup>-1</sup> ]	$6.91 \cdot 10^{-2}$ [cm <sup>-1</sup> ]	$1.23 \cdot 10^{-1}$ [cm <sup>-1</sup> ]
<b>RCFT</b> [pcm/K]	(0)	+ 8	+ 4	- 6	(0)	(0)	0	(0)	(0)
<b>RCCT</b> [mk/K]	- 2	+ 3	- 2	- 3	- 7	- 2	+ 1	(0)	(0)

Tab. 2. Diffusion data of 17x17's zone 1 at HZP, with their Relative Changes vs. Fuel and Coolant Temperatures.

Only data of 17x17's zone 1 are given by Tab. 2, as an example. Compared to sub-moderated options, most differences are on  $v_1$  (increased by a factor of 3 in the 21x21 core) and  $\Sigma_{12}$  (strongly reduced to only  $0.4 \cdot 10^{-4}$  cm<sup>-1</sup> in the same case). In any case, for instance in the 17x17 core, all non-zero RCFT values do not change much (only  $\pm 1$  pcm/K) between fissile zones (1 to 3), even rodded. With zone 4 on the contrary, great differences are observed for instance on  $\Sigma_{a1}$ 's and  $v\Sigma_{f1}$ 's RCFT (of +13 and +4 pcm/K respectively). Such values are typical of zone 4, which only contains <sup>232</sup>Th at BOC. For REA, delayed neutron fractions are checked to remain constant (between 300 and 330 pcm in zones 1 to 3, while zone 4's ranges from about 1400 pcm in the 17x17 case up to 2600 pcm in the 21x21 case). Finally, for necessary HFP calculations, diffusion data are computed at ( $T_{fuel}$ ,  $T_{cool}$ ) = (900, 580) too.

### III.B. Adjusted thermal lumped assembly model

Sub-moderation down to a water-to-fuel volumic ratio as low as 0.8 in the 21x21 case (considered as the acceptable minimum with a standard PWR primary circuit) should cost a higher pressure drop and thus an increased coolant mass flow  $F_{cool}$  (by about 10%). Yet, for simplified comparison, the same value of 50 kg.s<sup>-1</sup> per FA (halved from N4-type value, since core height is reduced to 2 m) is imposed to all tested cores. Less efficient heat extraction in smaller channels is roughly compensated by the reduction of fuel volumic power (cf. Fig. 2), giving in all cases a similar  $T_{cool}$  gradient of about 40 K for each assembly. Let us note that corresponding values per unit area of 1.83, 2.25 and 3.02 ton.s<sup>-1</sup>.m<sup>-2</sup> are close to adapted values<sup>7</sup>, obtained via enthalpic balance with an imposed gradient of 40 K.

Our diffusion core model for NDM<sup>4</sup> is 2D, close for instance to the one used for the so-called mini-core benchmark<sup>5</sup> (extended to the bigger size of Fig. 1). For the reflector, a simple extrapolation distance (of about 3.5 cm) is used. The thermal lumped coupling<sup>5</sup> of each FA is described by Eqs. (1) and (2):

$$\rho_{fuel} V_{fuel} C_{fuel} \frac{dT_{fuel}}{dt} = P_{tot} - G_{fuel}(T_{fuel} - T_{cool}) \quad (1)$$

$$\begin{aligned} \rho_{cool} V_{cool} C_{cool} \frac{dT_{cool}}{dt} &= G_{fuel}(T_{fuel} - T_{cool}) \\ &- 2F_{cool}C_{cool}(T_{cool} - T_{in}) \end{aligned} \quad (2)$$

where  $\rho$ 's are densities,  $V$ 's are volumes,  $C$ 's are heat capacities in  $J \cdot kg^{-1} \cdot K^{-1}$ ,  $P_{tot}$  is the total power released in the considered lump (supposed to be only in fuel) in  $W$  and  $G_{fuel}$  is the global conductance of the fuel-to-coolant heat transfer. In  $W \cdot K^{-1}$ , the latter parameter is the only unknown and is estimated together with the HFP equilibrium, in the two main following steps which can be iterated.

The first step consists in the calculation of a first HFP equilibrium, starting from an initial guess version of the core with pre-computed diffusion data at  $(T_{fuel}, T_{cool}) = (900, 580)$  and a consistent initial value of  $G_{fuel} = (600 \cdot 10^6 / 69) / (900 - 580) \approx 2.7 \cdot 10^4 \text{ W} \cdot \text{K}^{-1}$  since only the 69 FAs of zones 1 to 3 have a non-zero power at BOC. Each FA's  $T_{cool}$  value is forced to equilibrium as the only unknown of merged Eqs. (1) and (2), giving a cubic equation due to the quadratic fit used for  $C_{cool}$  from NIST data<sup>15</sup>. Hence  $T_{fuel}$  first equilibrium value for each FA, followed by its 2-g neutron and (6-g) precursor numbers via NDM's IRIS (Iterative Recovery of Initial Stability) algorithm<sup>4</sup> which is kind of a simplified Source Iteration Method. Of course, temperature dependence of diffusion data is fully taken into account in this process.

The second step aims at obtaining, from HFP equilibrium, a refined value for  $G_{fuel}$  (still common to all FAs) with possible iteration (back to first step of coupled equilibrium calculation) until its convergence. Each FA is computed by SMURE's BATH<sup>3,6</sup> (Basic Approach to Thermal-Hydraulics) package, solving energy conservation equations in each of the 20 axial levels of an average channel with fuel, gap, cladding and coolant parts. More detailed than the lumped thermal model used at core scale, it uses a conducto-convective coefficient obtained from Nusselt number, itself estimated from the Dittus-Boelter correlation. This way, one pair  $(P, T_{fuel}-T_{cool})$  of power and average temperature gradient is obtained for each of the 17 different FAs of zones 1 to 4. Linear interpolation of these points gives new  $G_{fuel}$  values of  $3.8 \cdot 10^4$ ,  $5.2 \cdot 10^4$  and  $6.6 \cdot 10^4 \text{ W} \cdot \text{K}^{-1}$  for the 17x17, 19x19 and 21x21 cores respectively.

Back to first step, a second HFP calculation with the new  $G_{fuel}$  value leads to a very slight update of FA powers and temperatures, so that a second batch of BATH runs confirms convergence. Tab. 3 shows obtained HFP equilibria, with maximal powers of about 10 MW in east of zones 2 and 3. Via its BATH axial details, each FA of zones 1 to 3 is checked to have an output  $T_{cool}$  below boiling point (of about 610 K) while all zone 4's remain at  $T_{in}$  (560 K). Maximal value is 605 K, reached in 17x17's E[3].

		(a) 17x17 core @HFP (BOC)			(b) 19x19 core @HFP (BOC)			(c) 21x21 core @HFP (BOC)		
		NE[2][2]	8.49 MW	799 K	NE[2][2]	8.11 MW	732 K	NE[2][2]	7.94 MW	696 K
FA name										
FA power										
$T_{fuel}$ (avg)										
$T_{cool}$ (avg)										
		NE[1][1]	9.30 MW	8.61 MW	NE[1][2]	8.04 MW	NE[1][3]	7.66 MW	NE[1][2]	8.83 MW
		822 K	803 K	787 K	722 K	729 K	711 K	9.56 MW	NE[1][3]	9.30 MW
		577.7 K	576.5 K	575.4 K	577.9 K	575.4 K	576.8 K	7.96 MW	719 K	719 K
		NE[0][0]	7.40 MW	7.71 MW	NE[0][1]	9.42 MW	NE[0][2]	8.00 MW	NE[0][1]	685 K
		769 K	778 K	778 K	826 K	843 K	826 K	7.95 MW	726 K	726 K
		574.3 K	574.8 K	574.8 K	577.9 K	578.9 K	578.9 K	9.83 MW	578.1 K	578.3 K
Center	E[0]	E[1]	E[2]	E[3]	Center	E[0]	E[1]	E[2]	E[3]	E[3]
7.20 MW	7.31 MW	7.67 MW	9.66 MW	10.62 MW	7.44 MW	7.56 MW	7.95 MW	9.83 MW	10.29 MW	777 K
763 K	766 K	776 K	832 K	859 K	717 K	720 K	728 K	768 K	777 K	777 K
573.9 K	574.1 K	574.8 K	578.3 K	579.9 K	574.6 K	574.6 K	575.3 K	578.6 K	579.3 K	579.3 K

Tab. 3. Main results obtained for the HFP equilibria at BOC by our 2D thermal lumped NDM (E-NE octants only).

## **IV. Simple rod ejection accidents from HZP**

The HFP equilibrium of each core has just been entirely characterized, so that it is now possible to use a simple and single criterion from it for our preliminary safety assessment based on REA from HZP. This criterion is that no FA-averaged coolant temperature should exceed its HFP value. This implicitly accounts for conservative margins towards boiling (without any need for DNB calculation though), and allows easy comparison too via the minimal difference (between the maximal FA coolant temperature during transient and its HFP value) of each core. After giving more details about main approximations and REA scenarios, our main results and first conclusions are given for all compared cores.

### **IV.A. Main approximations and REA scenarios**

Same thermal lumped 2D NDM than previously described for HFP calculation is used for transient calculations. Let us specify that this simple version has already been checked in a so-called mini-core REA benchmark<sup>5</sup> to slightly overestimate FA powers compared to a more refined 3D version, and is used conservatively. A significative approximation deals with the homogenization of diffusion data in partially rodded FAs during REA. An ejected control cluster divides its FA into two sub-volumes which cannot be differentiated in 2D, making simple volume weighting (instead of proper weighting by the product of flux and volume) the only possible way for homogenization indeed.

Although no special effort was made towards minimization of computing time, 1 s of transient only takes about one hour on a single CPU (Intel Core i5-6500 at 3.2 GHz). Integration is performed within a fully explicit scheme by a classical fourth-order Runge-Kutta method, using a typical step of  $10^{-6}$  s (small enough compared to generation times of about 9, 5 and  $3 \cdot 10^{-6}$  s at BOC for the 17x17, 19x19 and 21x21 cores respectively). Let us specify that generation time  $\Lambda$ , essential in point kinetics, is no NDM parameter and is simply rebuilt from cross sections. Still,  $\Lambda$  is our main conservative argument for choosing BOC which minimizes it (e.g. in the 17x17 case,  $\Lambda$  increases from  $9 \cdot 10^{-6}$  s at BOC up to  $1.4 \cdot 10^{-5}$  s at EOC), while delayed neutron fractions remain almost constant. Now starting from HZP at BOC, the extrapolation distance (used as a basic reflector model) is slightly reduced to 3.3 cm.

As previously described in III.A, ejected so-called control rods are clusters of 24 B<sub>4</sub>C rods (PWR-like<sup>14</sup>, except a 90 at% enrichment of B in <sup>10</sup>B). Three scenarios are considered, with the complete ejection in 0.05 s (halved from PWR standard since core height is reduced to 2 m) of:

- a. one rod fully inserted at BOT (Beginning Of Transient) in NE[1][1] (“one-rod” ejection),
- b. two rods, in NE[1][1] and its symmetric NW[1][1] about the y-axis (“two-rod” ejection)
- c. and finally four rods, in all [1][1] FAs (“four-rod” ejection).

The calculation of diffusion data and their relative changes vs. temperatures (detailed in III.A) gives as by-product the estimated total reactivity worth per rod (supposing an instantaneous ejection, with no thermal feedback) for each core. Decreasing with spectrum hardening, such a (maximal) worth ranges from about 1200 pcm per rod in the 17x17 case down to 900 pcm per rod in the 21x21 case.

### **IV.B. Comparative analysis as design transients**

A first check to be made on Fig. 5 (showing main one-rod ejection results) is that in all cases maximal reactivity insertion is above the previously estimated worth (a), because its differential value is higher during the transient (as well-known maximal at mid height). Only in the 17x17 case is reached Point Of Adding Heat (POAH) after the end of ejection, with a  $3.0 \cdot 10^5$  MW power peak at  $t = 0.053$  s (b). Due to smaller generation times, power peaks are higher in the 19x19 ( $4.4 \cdot 10^5$  MW) and 21x21 ( $4.7 \cdot 10^5$  MW) cases. For the same reason, POAH’s are reached about 0.005 s sooner in these cases (c). Final T<sub>fuel</sub> values are logically all the lower as lattice is tight and fuel inventory high. Back to (a), the 17x17 case exhibits the strongest thermal feedback with a quite long undershoot (a’). Highest T<sub>fuel</sub> (of about 830 K) in this case is reached at  $t = 0.058$  s in NE[0][3], yet only NE[1][1] is used in the following. As regards our criterion, all three cases appear equivalent (c’) with the same maximal T<sub>cool</sub> of 573 K for NE[1][1] (i.e. “-5 K” below its HFP value of 578 K). All other FAs have been checked to behave the same way.

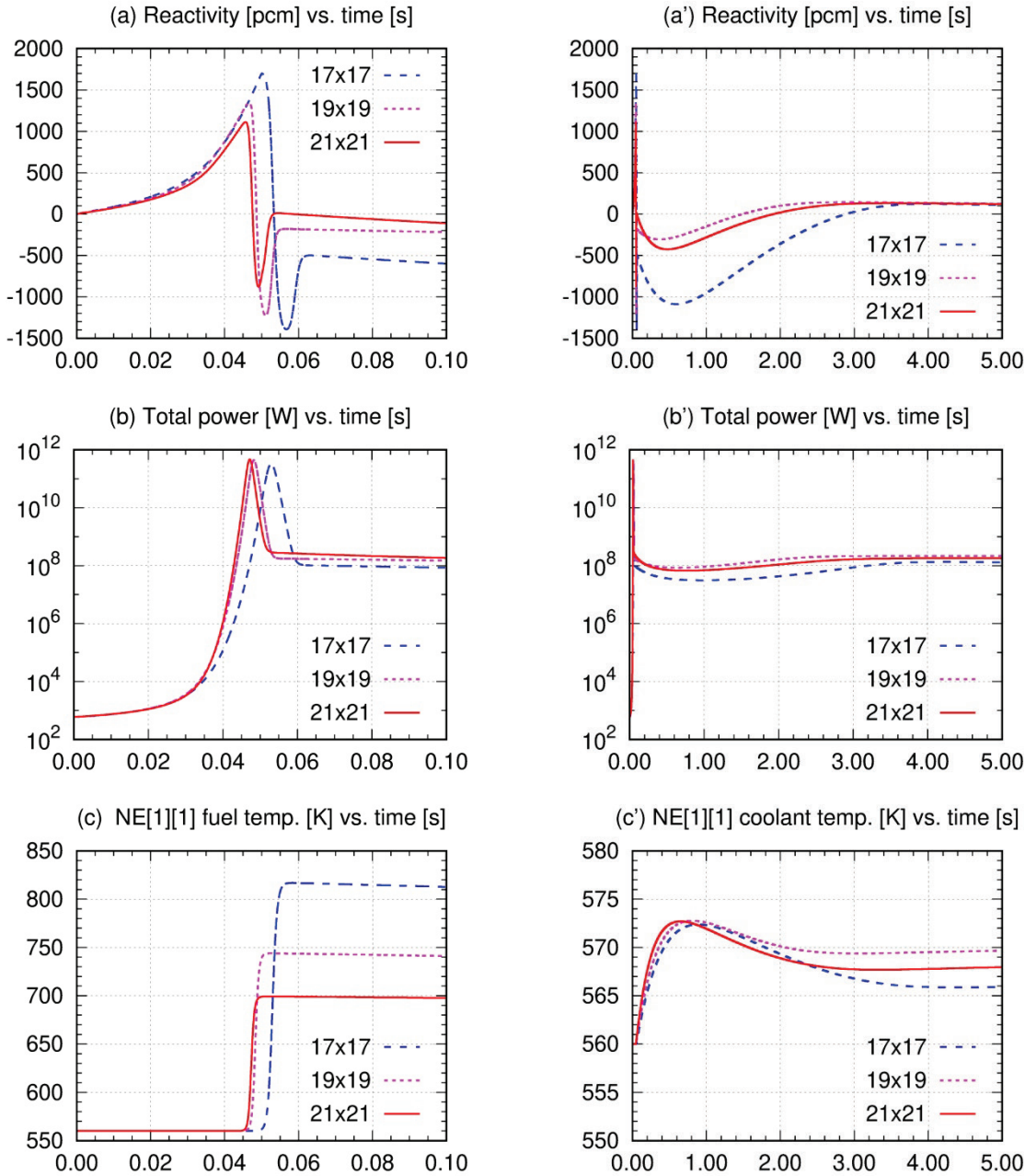


Fig. 5. Main results obtained on one-rod ejection from HZP in the three cases, compared over 0.1 s and 5.0 s.

Fig. 6(a) shows that maximal reactivity insertions have about same values in two-rod than in one-rod transients, with faster insertion rates though. Hence POAH's are advanced by about 0.01 s (c). In the 17x17 case, this leads to a similar behaviour with an even lower maximal  $T_{cool}$  value (c') of 571 K for NE[1][1]. For other cases, this unique criterion is on the contrary degraded, but still acceptable. These cases exhibit two thermal feedbacks (a) and power peaks (b), first ones occurring way before the end of ejection (around  $t = 0.035$  s) and thus leaving time for extra reactivity insertion afterwards. In the 19x19 case,  $T_{cool}$  reaches its maximal value (c') of 576 K ("−2 K" vs. HFP) at EOT (End Of Transient), which can be considered as an aggravating factor. In the 21x21 case, margin vs. HFP is cancelled out (with a maximal  $T_{cool}$  of 578 K around  $t = 0.6$  s) but EOT's value is lower ("−4 K" vs. HFP), which makes both safety levels similar from the restricted point of view of our single criterion. Such a tight margin calls for more detailed studies, with proper DNB calculations. As a final remark, the 17x17 core is still passing four-rod ejection ("−2 K" vs. HFP around  $t = 0.9$  s), while all FAs (zones 1 to 3) of other cases see their  $T_{cool}$  values at EOT exceeding HFP by +3 to +5 K (e.g. 583 K for NE[1][1] in all cases).

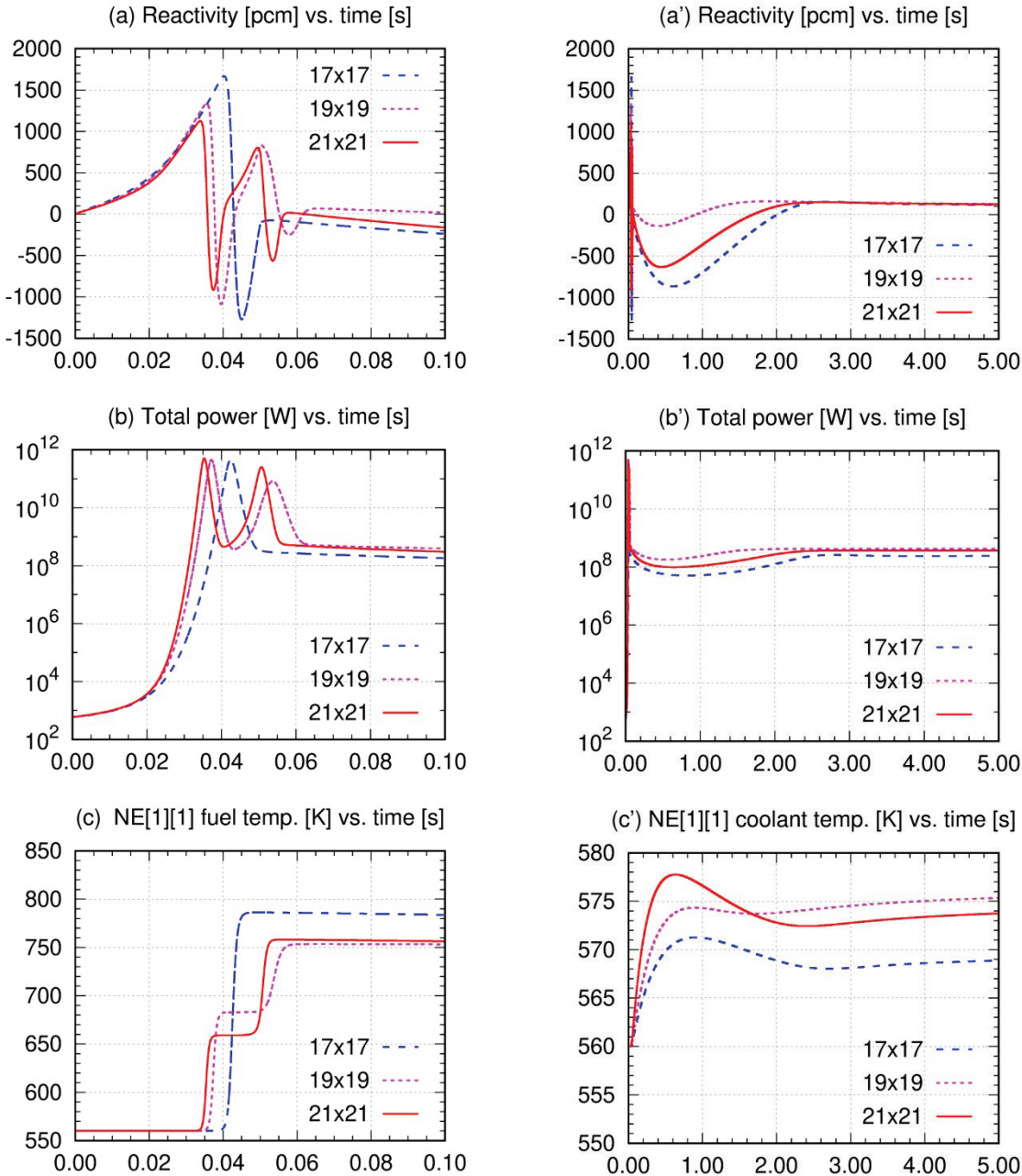


Fig. 6. Main results obtained on two-rod ejection from HZP in the three cases, compared over 0.1 s and 5.0 s.

## V. Conclusions and perspectives

The KNACK toolbox of simple academic methods has given us access to both conversion and safety assessment of thorium-fueled SMR cores operated by D<sub>2</sub>O/H<sub>2</sub>O SSC. Using Serpent 2 with a few evolving rings of FAs, it has shown on one hand the great potential of D<sub>2</sub>O as a coolant in tight lattices. Using NDM (conceived for a high “accuracy vs. complexity ratio”), it has pointed out on the other hand the limits of such lattices, with thermal-hydraulic issues which our future studies will try to mitigate.

The 21x21 conversion performance of the D<sub>2</sub>O/H<sub>2</sub>O SMR analyzed here is all the more interesting as it almost mimics the famous LWBR proof-of-breeding<sup>1</sup> from thorium fuel in a strongly sub-moderated and power-deterred H<sub>2</sub>O-cooled core, reaching 1.01 as FIR after 5 (interrupted) years of operation at 240 MW<sub>th</sub>. The D<sub>2</sub>O/H<sub>2</sub>O SSC solution gives thus access to the same kind of conversion regime, but in a more classical PWR-like SMR core (of 600 MW<sub>th</sub>) and with technical issues which appear much less challenging (provided that fuel and cladding can endure irradiation during its 5-y single batch).

As for safety, sub-moderated cases are unsurprisingly the most limiting against REA and boiling crisis. Yet, these cases are sufficiently not too degraded compared to standard lattice to justify further DNB calculations, especially focused on the promising 21x21 case which moreover seems to benefit from its higher fuel content and thermal inertia. Dedicated adjustments, like a higher coolant mass flow  $F_{cool}$  (more adapted than the unique value chosen in this work for sake of comparison) and/or a bigger core height, could help to improve heat extraction from this tight lattice during such demanding transients as REA. Other unprotected reactivity insertion scenarios should be evaluated and eventually promoted to the rank of design transient. For instance, the core could be flooded with  $H_2O$  in a few seconds<sup>10</sup>. Static calculations show that  $k_{eff}$  increases up to 1.5 in all cases by instantaneous replacement of  $D_2O$ , which of course is not realistic and calls for injection models either based on discrete pre-tabulated concentration fields or directly on CFD (like in boron-dilution accidents for  $H_2O$ -cooled cores).

Because of the complexity of  $D_2O$  dilution (and tritium removal) systems going with  $D_2O/H_2O$  SSC, the final proportion of  $H_2O$  in coolant has to be reduced as much as possible. More flexible than  $Gd_2O_3$ ,  $ZrB_2$  coatings could be used with optimized  $^{10}B$  enrichment, thickness and localization for each FA. To maximize burnup, lattice zoning could be performed (from 21x21 in zone 1 to 17x17 in zone 4, so that power is still flattened but with a reduced initial fissile inventory). For the same purpose, blanket re-use (ideally without reprocessing) could be profitably investigated. Once an optimal core image is reached as regards conversion and safety, a Th/Pu version will be adapted to answer the transition question.

## References

- 1) A. Nuttin, P. Guillemin et al., "Comparative analysis of high conversion achievable in thorium-fueled slightly modified CANDU and PWR reactors," *Annals of Nuclear Energy*, **40**, 171-189 (2012).
- 2) J. Leppänen et al., "User manual of the Monte Carlo code Serpent 2," <serpent.vtt.fi/mediawiki> (2015).
- 3) O. Méplan et al., "SMURE, a Serpent-MCNP Utility for Reactor Evolution," Computer Program Services of OECD Nuclear Energy Agency and <ipsc.in2p3.fr/MURE/html/SMURE/UserGuide> (2015).
- 4) A. Nuttin, P. Prévot et al., "Validation of the minimalistic Nodal Drift Method for spatial kinetics on a simple CANDU LOCA benchmark," *Annals of Nuclear Energy*, **88**, 135-150 (2016).
- 5) P. Prévot, A. Nuttin et al., "Enhancements to the Nodal Drift Method for a Rod Ejection Accident in a PWR-like mini-core with lumped thermal model," *Annals of Nuclear Energy*, **101**, 128-138 (2017).
- 6) P. Prévot, A. Nuttin, N. Capellan et al., "Preliminary design studies by a complete academic simulation toolbox of a water-cooled thorium-fueled Small Modular Reactor core," In: *Proc. Int. Conf. GLOBAL 2017*.
- 7) P. Prévot, "Développement d'outils académiques pour la conception de réacteurs innovants, application à des SMR refroidis à l'eau légère et chargés en thorium," PhD thesis, UGA (2018).
- 8) M.C. Edlund and G.K. Rhode, "Spectral Shift Control," *Nucleonics*, **16**, 80-81 (1958).
- 9) N. Brown and A. Worrall, "Fuel cycle performance of thermal spectrum Small Modular Reactors," In: *Proc. Int. Conf. ICAPP 2016*
- 10) B.A. Lindley and G.T. Parks, "The Spectral Shift Control Reactor as an option for much improved uranium utilisation in single-batch SMRs," *Nucl. Eng. Design*, **309**, 75-83 (2016).
- 11) E. Kitcher and S. Chirayath, "Neutronics and thermal-hydraulics analysis of a small modular reactor," *Annals of Nuclear Energy*, **97**, 232-245 (2016).
- 12) M. Lung and O. Gremm, "Perspectives of the thorium fuel cycle," *Nucl. Eng. Design*, **180**, 133-146 (1998).
- 13) F. de Waegh, "BR3/Vulcain core performance: theoretical and experimental aspects," In: Proc. Symposium on heavy-water power reactors held by the IAEA in Vienna (1967).
- 14) T. Kozlowski and T. Downar, "PWR MOX/UO<sub>2</sub> Core Transient Benchmark," Final Report NEA-6048, OECD Nuclear Energy Agency (2007).
- 15) NIST, Thermophysical Properties of Fluid Systems, <webbook.nist.gov/chemistry/fluid> (2011).